Journal of Arid Environments (2003) **54**: 395–404
doi:10.1006/jare.2002.1098

Influence of timing and spatial extent of savanna fires in southern Africa on atmospheric emissions

Stefania Korontzi★*, Christopher O. Justice★ & Robert J. Scholes†

★*Department of Geography, University of Maryland, College Park MD 20742, USA*
†*Environmentek, CSIR, P.O. Box 395, Pretoria 0001, South Africa*

(Received 15 July 2000, accepted in its final form 30 August 2001)

Biomass burning is an important ecosystem process in southern Africa, with significant implications for regional and global atmospheric chemistry and biogeochemical cycles. In this paper, representative Landsat path-row scene locations, distributed over southern Africa, were used to quantify the area burned and to understand the coupled role of the timing and the extent of burning on regional emissions. The total area burned and the scar size distribution were found to vary between semi-arid and humid scenes and dry and average rainfall years. Analysis of images from the start and end of the burning season resulted in a modest underestimate of the annual area burned, as compared to using a monthly time-series approach. However, at the regional level the start/end method is likely to yield acceptable annual burned area estimates and total carbon dioxide estimates. On the other hand, combustion factors and emission factors vary sufficiently during the burning season to result in large errors in emission estimates of products of incomplete combustion, when using the start/end method. This study indicates that in southern Africa, the timing in addition to the extent of burning must be considered and that time-series satellite burned area products are needed to quantify pyrogenic emissions accurately.

Keywords: savanna fires; southern Africa; pyrogenic emissions; burned area; Landsat; Kalahari

Introduction

The first global satellite fire product from the Advanced Very High Resolution Radiometer (AVHRR) data (Stroppiana *et al.*, 2000) showed that the African continent has the highest occurrence of vegetation fires, found predominantly in savanna regions (Dwyer *et al.*, 2000). The majority of fires in southern Africa occur during the dry season, from May to October. Fires are found throughout the Kalahari

*Corresponding author. Tel: +1 301 403 8192; Fax: +1 301 314 9299. E-mail: stef@hermes.geog.umd.edu.

0140-1963/03/020395 + 10 $30.00/0

sand basin and are an important determinant of savanna structure and composition. Fire is also a significant source of trace gases and aerosols from savannas and the Kalahari region is likely to contribute significantly to regional pyrogenic emissions. In addition, fire is believed to play an important role in the carbon and nitrogen cycling in the Kalahari region (IGBP, 1997).

In the context of the International Panel on Climate Change (IPCC), scientists are studying the quantities of biomass burned, trace gas and aerosol emissions for southern Africa (Braatz *et al.*, 1995). The quantitative expression commonly used to estimate emissions of a given fire product (M) is

$$M = A \times F \times C \times E \qquad \text{(Eqn 1)}$$

where A is the burned area, F is the fuel loading, C is the combustion factor, characteristic of the completeness of combustion, and E is the emission factor, characteristic of the amount of the specific atmospheric species produced during the combustion (Hao *et al.*, 1996; Scholes *et al.*, 1996*a*; Barbosa *et al.*, 1999*a*). Emission estimates relying on remote sensing for A are much lower than those based on anecdotal estimates of A (Hao *et al.*, 1990; Hao and Liu; 1994; Scholes *et al.*, 1996*a*). The annual burned area is among the variables introducing large uncertainty in emissions modeling (Barbosa *et al.*, 1999*b*). Current efforts are focused on developing regional burned area satellite products (Roy *et al.*, 1999; Barbosa *et al.*, 1999b; Piccolini *et al.*, 2000).

In this paper, fire is studied for average and dry rainfall years along a rainfall gradient representative of the strong climatic gradient, from the arid south to the humid north, that exists in the Kalahari environment. Temporal resolution requirements for burned area information, driven by the need for accurate pyrogenic emissions quantification, are assessed. Seasonal emissions trends are simulated for varied spatial extent of burning in a grassland environment.

Methodology

In this study, Landsat data were used to estimate the burned area for 12 path-row scene locations in 1989 and six scene locations in 1992, distributed over southern Africa (Fig. 1). Burn scars were visually mapped on 1:250,000 Landsat multi-spectral scanner (MSS) false color composite prints (red = band 4, green = band 3, blue = band 2) and digitized. The minimum mapping unit was 180 m. For each Landsat scene, a difference image was derived from two images from the beginning and the end of the burning season. This difference image has been assumed to depict the annual area burned (Scholes *et al.*, 1996*b*). This method will be referred to as the start/end method.

To test the accuracy of the start/end method, a time-series analysis was performed for three scenes located in humid areas, where burn scars were expected to be the most transient due to the flush of green vegetation following burning. The new area burned between each image and its preceding image was mapped on five Landsat images per path-row scene location, covering the fire season, spaced about a month apart. This is termed the time-series method. The start/end method slightly underestimated (8–12%) the total area burned compared with the time-series method. The difference was attributed to rapid post-burn regrowth. Because most of the fire scars remained visible throughout the fire season, the start/end method was used for the total burned area analysis.

To compare emissions calculated from the two methods used to derive burned area, time-series images were analysed for 1989 (a normal precipitation year) for a scene comprised largely of dambo grassland, using Eqn (1). A dambo is a particular type of

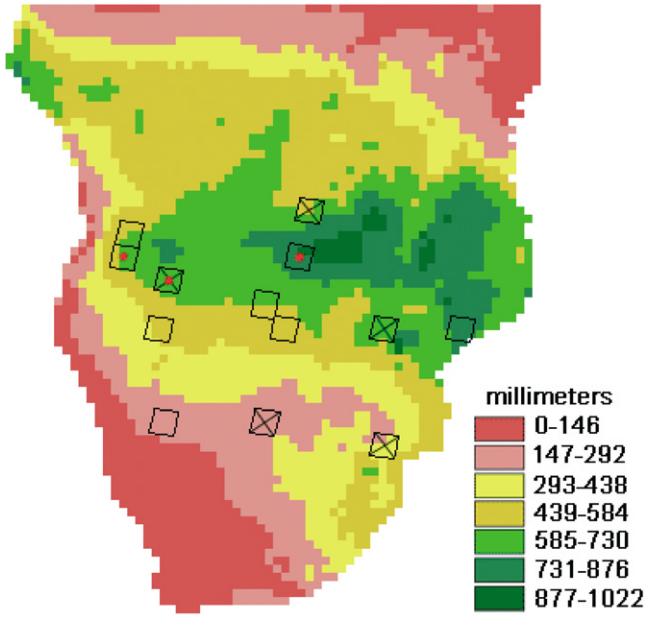

Figure 1. Location of study sites overlayed on a long-term mean annual rainfall map derived from data by New *et al.* (1999). Scenes marked with an x show sites for which both 1989 and 1992 data were analysed. Scenes marked with a red dot show sites for which time-series of data were analysed.

African grassland which is seasonally flooded during the wet season. The seasonal F and C values were retrieved from Hoffa *et al.* (1999). These measurements were sampled at prescribed burning plots that were successively burned weekly or biweekly between June and August 1996. The biomass amounts reported by Hoffa *et al.* fall within the normal range of fuel loadings for a dambo in an average rainfall year at an annually or biannually burned site (Shea *et al.*, 1996; Stocks *et al.*, 1996). Therefore, the seasonal values of F and C were deemed as representative for the 1989 dambo grassland location studied here. Seasonal E's algorithms were derived from late dry season raw E data by Ward *et al.* (1996) and seasonal modified combustion efficiency data (MCE, the ratio of carbon emissions as CO_2 to carbon emissions as CO_2+CO) from Hoffa *et al.* for carbon dioxide (CO_2), carbon monoxide (CO), methane (CH_4), nonmethane hydrocarbons (NMHC), and fire particulate matter (PM2·5) (Table 1). To obtain estimates of the amount of the above atmospheric species with the time-series method, we applied the calculated E of Table 1 to the biomass burned. To quantify emissions with the start/end method we used the mean F and the late dry season C and E, which is the way traditionally researchers have calculated emissions (Scholes *et al.*, 1996a; Andreae, 1997; Barbosa *et al.*, 1999*a*,*b*).

Table 1. *Seasonal emission factors for the dambo grassland*

Emission factors ($g\,kg^{-1}$)	June	July	August	September
E_{CO_2}	1586	1650	1734	1755
E_{CO}	138	104	58	46
E_{CH_4}	5·8	4·0	1·5	0·8
E_{NMHC}	5·2	3·8	2·0	1·5
$E_{PM2·5}$	9·7	7·1	3·6	2·7

Furthermore, a simulation analysis was performed for the same dambo grassland scene to assess the possible contributions of early and late dry season burning to the total emissions. This is an important question from a fire management perspective since controlled early burning is a common natural resources management tool in the African region, used to prevent degrading effects in the various ecosystems that are caused by high-intensity late season fires (Chidumayo, 1988; Frost, 1996). The simulation was done by varying the area burned for different scenarios of early and late dry season burning and calculating the resulting total emissions. For this particular simulation study, the early and late dry season pyrogenic emissions were calculated using the E, F, and C values for June and September, respectively.

Results and discussions

Burned area

Differences in the total area burned and the scar size distribution were found between semi-arid and humid scenes in 1989. A slightly larger percentage of the total scene area was burned in semi-arid grasslands (12%) than in humid miombo woodlands (9%). In semi-arid areas there was a greater number of fires burning larger than 1 km^2 in size, whereas in the more humid areas smaller fire scars ($<1\,km^2$ area) were predominant (Fig. 2). An example of the appearance of the fire scars in the different ecosystems is presented in Fig. 3(a,b). In the semi-arid areas a few very large fires ($>100\,km^2$ in size) accounted for about 60% of the total burned area (Fig. 4(a)). In the humid areas, even though about 70% of the scars were $<1\,km^2$, they comprised only 12% of the total area burned (Fig. 4(b)). It should be noted that the size range categories shown in the graphs were deliberately chosen to correspond to the spatial resolution of the 250 m, 500 m, and 1 km MODIS channels, which are candidate spatial resolutions for the MODerate resolution Imaging Spectroradiometer (MODIS) burned area products. Our findings indicate that burned area mapping at a resolution of 1 km^2 would satisfy regional information requirements for burned area.

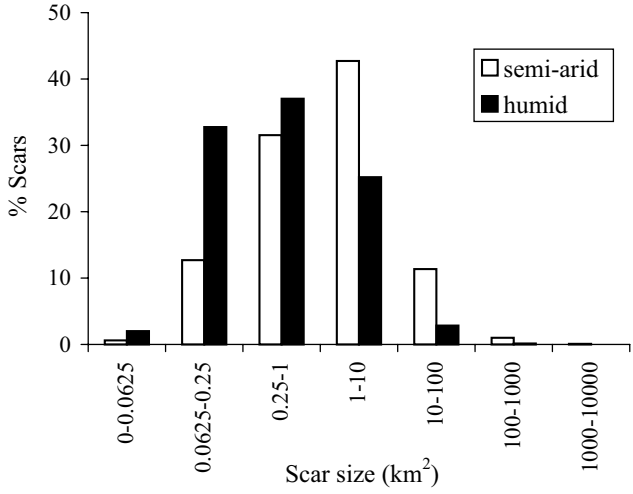

Figure 2. Scar size distribution for the 1989 burned areas.

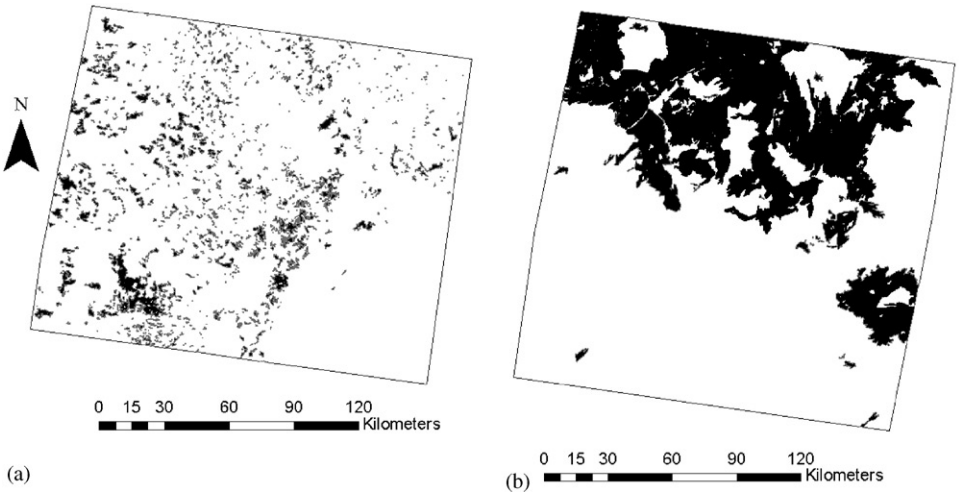

Figure 3. Fire scar appearance at two areas with different climatic conditions in 1989: (a) humid site in Mozambique; (b) semi-arid site in Botswana.

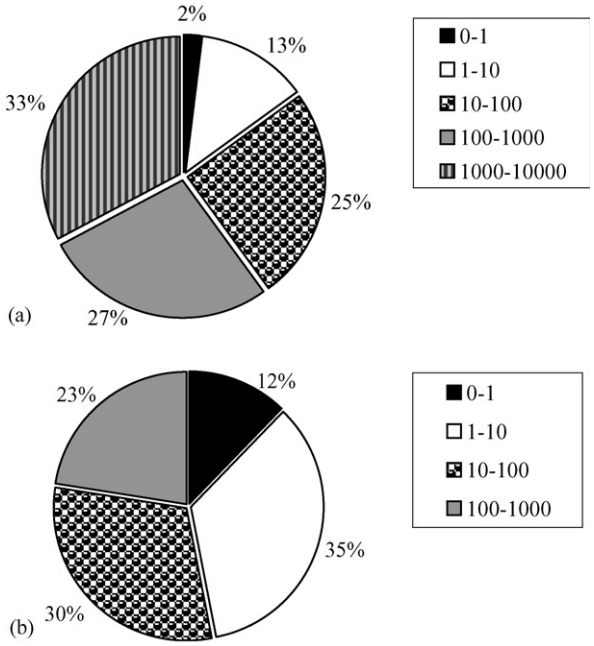

Figure 4. Percentage of the total area burned in each scar size category (km^2) for the 1989 scenes: (a) semi-arid; (b) humid.

The 1992 fire season (May–October) followed an exceptionally dry summer throughout southern Africa. Differences in the total area burned, the scar size distribution and the amount burned in each fire size range were observed between 1992 and an average rainfall year (1989). Comparison of three semi-arid scenes from the two years showed that in 1992 the regional drought resulted in a decrease in the burned area by a factor of 10. In 1992, a decline in the number of larger sized burn

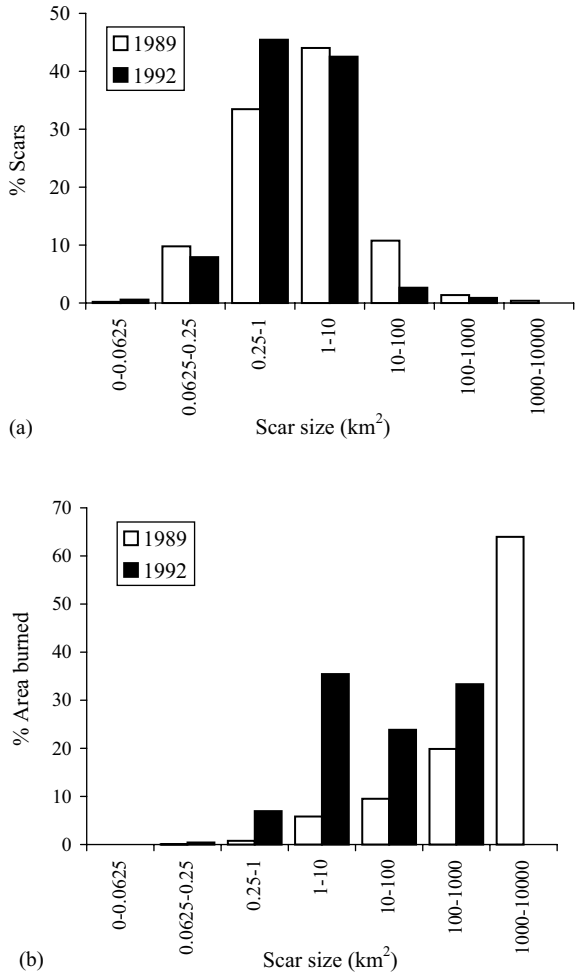

Figure 5. Comparison of the same three semi-arid scenes for 1989 and 1992; (a) scar size distribution; (b) percentage area burned in each scar size category.

scars was observed with an 11% increase in scars $<1\,km^2$ (Fig. 5(a)). In 1989, a small number of very large fires $>1000\,km^2$ accounted for the majority of the burned area, whereas in 1992 there was an absence of fires $>1000\,km^2$ and the burning was more evenly distributed among the three smaller scar size ranges between 1 and $1000\,km^2$ (Fig. 5(b)). Our data support the hypothesis that drought reduces fuel load abundance and the extent of burning in semi-arid regions (Justice *et al.*, 1996). In 1992 there was a shift to larger sized scars in humid areas as compared to 1989 (Figs 2 and 6). This could be attributed to the drying out and increased flammability of the fuel because of the reduced rainfall in the normally humid areas.

Pyrogenic emissions

The time-series method was used as the reference for the actual biomass burned and emission estimates. For the particular dambo scene, the start/end method underestimated the true area burned by 12%. Serendipitously, this underestimate of the

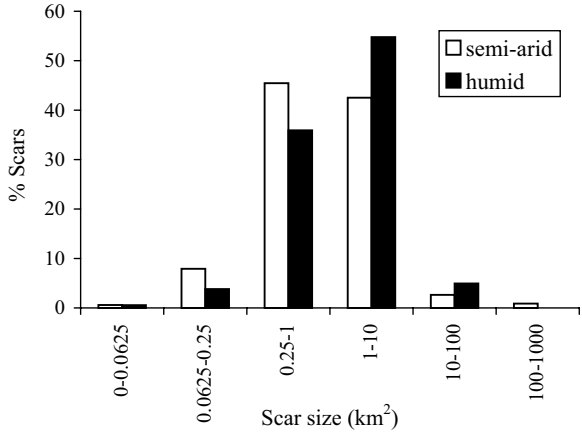

Figure 6. Scar size distribution for the 1992 burned areas.

area burned gave an overestimate of the biomass burned (12%) as compared to the time-series analysis. This overestimation was attributed to an almost even temporal distribution of burning (20% May–June, 24% June–July, 24% July–August, 32% August–September) and seasonally variable C's. A simulation done by varying the amounts of burning showed that the start/end method representing 100% of the area burned would overestimate the biomass burned by 22%. To get equal amounts of biomass burned by the two methods, the start/end method would have to underestimate the true area burned by 21%.

Distinct differences in the calculated emissions were also found between the two methods. The start/end method underestimated emissions of products of incomplete combustion relative to the time-series method (Table 2). Considering that the start/end method also overestimates the biomass burned, the underestimation error in the emissions is likely even larger than presented here. These results highlight the shortcoming of the start/end method in accounting for the seasonal variations of the area burned, E and C in the emissions calculations. In the case of CO_2, a slight overestimation occurs with the start/end method which though at the regional level is not deemed important. This is thought to be the result of the smaller seasonal variability of the CO_2 E's as compared to the E's of products of incomplete combustion (Table 1). It should also be noted that in this region of the world, the existing E's algorithms for the different pyrogenically produced atmospheric species are derived from late dry season measurements. Therefore, the validity of extrapolating to early dry season burning E's is not known. Obviously, seasonal measurements of E's are necessary to test this.

Table 2. *Total pyrogenic emissions for the dambo grassland using the time-series and start/end methods*

Emissions (Gg)	Time-series method	Start/end method	Relative error %
CO	257·56	167·68	−54
CH_4	8·61	3·09	−179
NMHC	9·30	5·62	−65
PM2·5	16·95	9·72	−74
CO_2	5493·60	6400·57	14

Table 3. *Temporal variation of pyrogenic emissions as a function of timing and amount of burning and contribution (%) of early and late emissions to the total emissions for each atmospheric species*

Emissions	Percentage of early/late dry season burning					
	95/5	75/25	50/50	35/65	15/85	5/95
Total CO (Gg)	298	267	220	188	157	141
% early CO	97·8	87·4	69·8	55·4	28·9	10·8
% late CO	2·2	12·6	30·2	44·6	71·1	89·2
Total CH_4 (Gg)	12·4	11·6	9·6	8·0	5·2	2·8
% early CH_4	99·1	95	87·9	81·1	62·1	22·7
% late CH_4	0·9	5	12·1	18·9	37·9	77·3
Total NMHC (Gg)	11·3	9·8	8·0	6·9	5·5	4·7
% early NMHC	98·1	88·9	72·7	58·9	32	12·3
% late NMHC	1·9	11·1	27·3	41·1	68	87·7
Total PM2·5 (Gg)	20·4	18·9	14·8	12·7	9·9	8·5
% early PM2·5	98·1	89·2	73·4	59·8	32·8	12·7
% late PM2·5	1·9	10·8	26·6	40·2	67·2	87·3
Total CO_2 (Gg)	3617	3932	4246	4561	4875	5033
% early CO_2	93	67·6	41	27·2	10·9	3·5
% late CO_2	7	20·3	43·7	59	89·1	96·5

To explore further the interplay of the timing and the extent of burning, *E*'s and *C*'s, a simulation analysis was performed for the same dambo grassland scene (Table 3) by varying the amount of burning for different scenarios of early and late dry season burning and calculating the resulting total emissions. If most of the burning (95%) occurred at the beginning of the season, this would significantly increase the total amounts of incomplete combustion products emitted (CO by a factor of 2, the total CH_4 by a factor of 4, the total NMHC by a factor of 2·4, and the total PM2·5 by a factor of 2·5). If most of the burning occurs at the end of the season, the timing and amount of burning rather than the *C* and *E* are the primary controlling factors on emissions (Tables 1 and 3). If the burning is more evenly distributed throughout the season, then *C* and *E* will exert the largest influence on the resulting emissions and both the early and late season burning would contribute significantly to the total emissions of incomplete combustion products.

Analysis of the 1992 AVHRR active fire product (Giglio *et al.*, 1999) showed that approximately 30% of all fires occurred in the early dry season (May–June). The time-series analysis of another grassland scene showed again that the burning was fairly evenly distributed throughout the season (19% May–June, 51% June–July, 30% July–September), whereas in a miombo woodland scene most of the burning occurred at the end of the dry season (2·4% May–June, 3·6% June–July, 13% July–August, 81% August–September). This indicates that early season fires could account for a significant portion of the total incomplete combustion compounds emitted during the dry season, at least in grassland ecosystems (Table 3). In the case of CO_2, where seasonal *E*'s are less variable, early *vs* late burning does not appear to have a large effect on the total emissions.

It is also important to bear in mind that the values of the input parameters to the emissions calculations used in this study fall within their normal ranges in an average precipitation year. Extrapolating the results to years with above- or below-average precipitation requires a dynamic modeling approach that can simulate the effects of

inter-annual climate variability, altered fire regimes and grazing pressure on these input variables. This further supports the need to move from a static modeling approach, such as the start/end method, to the development of spatially and temporally explicit regional emissions data sets.

Conclusions

In summary, our results demonstrate that incorporation of the temporal patterns of biomass burning in emissions modeling is important when assessing seasonal fluxes of trace gases and aerosols from savanna landscapes. Despite the slight underestimation of the total burned area with the start/end method as compared to a time-series approach, at the regional level the results are acceptably close. Similarly, the start/end method produces credible estimates of total CO_2 emissions as compared to the time-series method. In contrast, the intrinsic limitation of the start/end method to account for the temporal variations of fuel consumption and emission factors has a marked effect on the accurate quantification of pyrogenic emissions of products of incomplete combustion. The temporal distribution and amount of the burning will determine the type (i.e. products of complete *vs*. incomplete combustion) and quantities of biomass burning products emitted during the fire season. Time-series rather than annual burned area products are needed to drive increasingly sophisticated emissions models. The availability of fire information at suitable space-time-scales will enable improved understanding and prediction of the environmental impacts of pyrogenic emissions and strengthen natural resources management in the region.

We thank Dr Darold Ward for the useful discussions on emission factors.

References

Andreae, M.O. (1997). Emissions of trace gases and aerosols from southern African savanna fires. In: Van Wilgen, B.W, Andreae, M.O., Goldammer, J.G. & Lindesay, J.A. (Eds), Fire in Southern African Savannas, pp. 161–183. South Africa: Witwatersrand University Press. 24 pp.

Barbosa, P.M., Stroppiana, D., Gregoire, J.-M. & Pereira, J.M.C. (1999*a*). An assessment of vegetation fire in Africa (1981–1991): burned areas, burned biomass, and atmospheric emissions. *Global Biogeochemical Cycles*, **13**: 933–950.

Barbosa, P.M., Gregoire, J.-M. & Pereira, J.M.C. (1999*b*). An algorithm for extracting burned areas from time-series of AVHRR GAC data applied at a continental scale. *Remote Sensing of Environment*, **69**: 253–263.

Braatz, B.V., Brown, S., Isichei, A.O., Odada, E.O., Scholes, R.J., Sokona, Y., Drichi, P., Gaston, G., Delmas, R., Holmes, R., Amous, S., Muyungi, R.S., De Jode, A. & Gibbs, M. (1995). African greenhouse gas emission inventories and mitigation options: forestry, land-use change, and agriculture. *Environmental Monitoring and Assessment*, **38**: 109–126.

Chidumayo, E.N. (1988). A reassessment of effects of fire in miombo regeneration in the Zambian Copperbelt. *Journal of Tropical Ecology*, **4**: 361–372.

Dwyer, E., Pinnock, S., Grégoire, J.-M. & Pereira, J.M.C. (2000). Global spatial and temporal distribution of vegetation fire as determined from satellite observations. *International Journal of Remote Sensing*, **21**: 1289–1302.

Frost, P. (1996). The ecology of miombo woodlands. In: Campbell, B. (Ed.), *The Miombo in Transition: Woodlands and Welfare in Africa*, pp. 11–58. Bogor, Indonesia: Center for International Forestry Research (CIFOR). 49 pp.

Giglio, L., Kendall, J. D. & Justice, C. O. (1999). Evaluation of global fire detection algorithms using simulated AVHRR infrared data. *International Journal of Remote Sensing*, **20**: 1947–1985.

Hao, W.M. & Liu, M.-H. (1994) Spatial and temporal distribution of tropical biomass burning. *Global Biogeochemical Cycles*, **8**: 495–503.

Hao, W.M., Liu, M.-H. & Crutzen, P.J. (1990). Estimates of annual and regional releases of CO_2 and other trace gases to the atmosphere from fires in the tropics, based on the FAO statistics for the period 1975–1980. In: Goldammer J.G. (Ed.), *Fire in the Tropical Biota: Ecosystem Processes and Global Challenges*, pp. 440–462. New York: Springer-Verlag.

Hao, W.M., Ward, D.E., Olbu, G. & Baker, S.P. (1996). Emissions of CO_2, CO, and hydrocarbons from fires in diverse African savanna ecosystems. Journal of Geophysical Research, **101**: 23,577–23,584.

Hoffa, E.A., Wakimoto, R.H., Ward, D.E., Hao, W.M. & Susott, R.A. (1999). Seasonality of carbon emissions from biomass burning in a Zambian savanna. *Journal of Geophysical Research*, **104**: 13,841–13,853.

International Geosphere–Biosphere Programme (IGBP) (1997). In: Scholes, R.J. & Parsons, D.A.B. (Eds), *The Kalahari Transect: Research on Global Change and Sustainable Development in Southern Africa*. IGBP Report 42. Stockholm, Sweden: Royal Swedish Academy of Sciences. 61 pp.

Justice, C.O., Kendall, J.D., Dowty, P.R. & Scholes, R.J. (1996). Satellite remote sensing of fires during the SAFARI campaign using NOAA Advanced Very High Resolution Radiometer data. *Journal of Geophysical Research*, **101**: 23,851–23,863.

New, M., Hulme, M. & Jones, P. (1999). Representing twentieth-century space–time climate variability. Part I: development of a 1961–90 mean monthly terrestrial climatology. *Journal of Climate*, **12**: 829–856.

Piccolini, I. & Arino, O. (2000). *Towards a Global Burned Surface World Atlas*. ESA Publication, ESTEC, Nooddwijk, Holland, *Earth Observation Quarterly*, **65**: 14–18.

Roy, D.P., Giglio, L., Kendall, J.D. & Justice, C.O. (1999). Multitemporal active-fire based burn scar detection algorithm. *International Journal of Remote Sensing*, **20**: 1031–1038.

Scholes, R.J., Ward, D.E. & Justice, C.O. (1996*a*). Emissions of trace gases and aerosol particles due to vegetation burning in southern hemisphere Africa. *Journal of Geophysical Research*, **101**: 23,677–23,682.

Scholes, R.J., Kendall, J. & Justice, C.O. (1996*b*). The quantity of biomass burned in southern Africa. *Journal of Geophysical Research*, **101**: 23,667–23,676.

Shea, R.W., Shea, B.W., Kauffman, J.B., Ward, D.E., Haskins, C.I. & Scholes, M.C. (1996). Fuel biomass and combustion factors associated with fires in savanna ecosystems of South Africa and Zambia. *Journal of Geophysical Research*, **101**(19): 23,551–23,568.

Stocks, B.J., Van Wilgen, B.W., Trollope, W.S.W., McRae, D.J., Mason, J.A., Weirich, F. & Potgieter, A.L.F. (1996). Fuels and fire bahavior dynamics on large-scale savanna fires in Kruger National Park, South Africa. *Journal of Geophysical Research*, **101**: 23,541–23,550.

Stroppiana, D., Pinnock, S. & Grégoire, J.-M. (2000). The Global Fire Product: daily fire occurrence from April 1992 to December 1993 derived from NOAA AVHRR data. *International Journal of Remote Sensing*, **21**: 1279–1288.

Ward, D.E., Shea, R.W., Kauffman, J.B., Justice, C.O., Hao, W.M., Susott, R.A. & Babbitt, R.E. (1996). Effect of fuel composition on combustion efficiency and emission factors for African savanna ecosystems. *Journal of Geophysical Research*, **101**: 23,569–23,576.